Downloaded from UvA-DARE, the institutional repository of the University of Amsterdam (UvA)
http://hdl.handle.net/11245/2.12963

File ID uvapub:12963
Filename 88707y.pdf
Version unknown

SOURCE (OR PART OF THE FOLLOWING SOURCE):
Type article - letter to the editor
Title The intensity distribution of faint gamma-ray bursts detected with BATSE
Author J.M. Kommers
Faculty FNWI: Astronomical Institute Anton Pannekoek (IAP)
Year 2000

FULL BIBLIOGRAPHIC DETAILS:
http://hdl.handle.net/11245/1.176113

Copyright

It is not permitted to download or to forward/distribute the text or part of it without the consent of the author(s) and/or copyright holder(s), other than for strictly personal, individual use.

UvA-DARE is a service provided by the library of the University of Amsterdam (http://dare.uva.nl)
(pagedate: 2014-08-14)

THE ASTROPHYSICAL JOURNAL, 533:696–709, 2000 April 20
© 2000. The American Astronomical Society. All rights reserved. Printed in U.S.A.

THE INTENSITY DISTRIBUTION OF FAINT GAMMA-RAY BURSTS DETECTED WITH BATSE

JEFFERSON M. KOMMERS,[1] WALTER H. G. LEWIN,[1] CHRYSSA KOUVELIOTOU,[2,3] JAN VAN PARADIJS,[4,5]
GEOFFREY N. PENDLETON,[4] CHARLES A. MEEGAN,[3] AND GERALD J. FISHMAN[3]
Received 1998 September 22; accepted 1999 March 1

ABSTRACT

We have recently completed a search of 6 years of archival BATSE data for gamma-ray bursts (GRBs) that were too faint to activate the real-time burst detection system running on board the spacecraft. These "nontriggered" bursts can be combined with the "triggered" bursts detected on board to produce a GRB intensity distribution that reaches peak fluxes a factor of ~ 2 lower than could be studied previously. The value of the $\langle V/V_{\max}\rangle$ statistic (in Euclidean space) for the bursts we detect is 0.177 ± 0.006. This surprisingly low value is obtained because we detected very few bursts on the 4.096 s and 8.192 s timescales (where most bursts have their highest signal-to-noise ratio) that were not already detected on the 1.024 s timescale. If allowance is made for a power-law distribution of intrinsic peak luminosities, the extended peak flux distribution is consistent with models in which the redshift distribution of the gamma-ray burst rate approximately traces the star formation history of the universe. We argue that this class of models is preferred over those in which the burst rate is independent of redshift. We use the peak flux distribution to derive a limit of 10% (99% confidence) on the fraction of the total burst rate that could be contributed by a spatially homogeneous (in Euclidean space) subpopulation of burst sources, such as type Ib/c supernovae. These results lend support to the conclusions of previous studies predicting that relatively few faint "classical" GRBs will be found below the BATSE onboard detection threshold.

Subject headings: gamma rays: bursts — methods: statistical

1. INTRODUCTION

The origin of some, and possibly all, gamma-ray bursts (GRBs) at cosmological distances has been firmly established with the identification of X-ray, optical, and radio afterglows (Costa et al. 1997; van Paradijs et al. 1997; Frail et al. 1997) and the subsequent measurement of cosmological redshifts for at least four of the optical afterglows and/or their host galaxies (Metzger et al. 1997; Kulkarni et al. 1998a; Djorgovski et al. 1998, 1999). The objects responsible for producing the majority of GRBs, the gamma-ray bursters themselves, have yet to be understood, however. To obtain an understanding of the spatial distribution of sources and the distribution of their burst luminosities is a crucial step toward identifying the physical processes that produce GRBs.

Before the rapid follow-up of GRB afterglows was made possible by the *BeppoSAX* satellite, the only way to test hypotheses about the spatial and luminosity distributions was to fit parametric models to the measured characteristics of the bursts themselves. For this purpose the distribution of GRB intensities was used (see, for example, Fenimore et al. 1993; Rutledge, Hui, & Lewin 1995; Fenimore & Bloom 1995; Cohen & Piran 1995; Hakkila et al. 1996, and references therein). The effects of cosmological time dilation on the time profiles of bright versus faint bursts were also studied (Norris et al. 1995). Since optical spectroscopic redshifts are so far associated with only four (possibly five) bursts,[6] number counts as a function of intensity remain an important tool for exploring the possible spatial and luminosity distributions of GRBs.

Several recent papers (Totani 1997, 1998; Wijers et al. 1998; Krumholz, Thorsett, & Harrison 1998; Mao & Mo 1998) have used the observed GRB intensity distributions to investigate the possibility that the redshift distribution of gamma-ray bursters traces the global star formation history of the universe. The motivation for this hypothesis is a collection of theoretical models in which GRBs are produced by stellar objects that evolve from their formation to their bursting phase on a timescale of ~ 100 Myr or less. This group of models includes the merging of a neutron star with another neutron star or a black hole, the collapse of a massive star, and the collapse of a Chandrasekhar-mass white dwarf (see Wijers et al. 1998 for references). In these scenarios, the cosmological redshift distribution of the GRB rate should approximately follow the redshift distribution of the formation rate of stellar objects; in other words, the GRB rate should trace the global star formation history of the universe. This hypothesis appears to solve some puzzling aspects of the observations, such as the "no host" problem (Schaefer et al. 1997; Wijers et al. 1998).

The star formation rate (SFR) as a function of redshift has been studied by Lilly et al. (1996), Fall, Charlot, & Pei (1996), Madau, Pozzetti, & Dickinson (1998b), and Hughes et al. (1998). The principal result of these studies is that the SFR was substantially higher in the past. Between the present and $z \approx 1$ the SFR increases by a factor of ~ 10; it

[1] Department of Physics and Center for Space Research, Massachusetts Institute of Technology, Cambridge, MA 02139; kommers@space.mit.edu.
[2] Universities Space Research Association, Huntsville, AL 35800.
[3] NASA/Marshall Space Flight Center, Huntsville, AL 35812.
[4] University of Alabama in Huntsville, Huntsville, AL 35812.
[5] University of Amsterdam, Amsterdam, Netherlands.

[6] The proposed association of GRB 980425 with SN 1998bw ($z = 0.008$; Galama et al. 1998) may indicate a separate class of GRBs (Bloom et al. 1998). We will therefore consider that event separately (see § 3.2).

peaks somewhere in the range $z \approx 1$ to $z \approx 3$; and it decreases to a rate comparable to the present by $z \approx 4$–5 (this last point remains uncertain).

Totani (1997), Wijers et al. (1998), Krumholz et al. (1998), and Mao & Mo (1998) all find that the GRB peak flux number counts can accommodate the hypothesis that the GRB rate follows the SFR. Among the important conclusions that these authors derive from this interpretation of the data are the following: (1) that the faintest gamma-ray bursts observed with the Burst and Transient Source Experiment (BATSE) on board the *Compton Gamma Ray Observatory* (*CGRO*) have already been produced at redshifts of $z \approx 3$ to $z \approx 6$ (Wijers et al. 1998; but see § 4); and (2) that more sensitive experiments are unlikely to discover large numbers of faint GRBs (of the "classical" kind that are detected with current instruments) below the BATSE onboard detection threshold. The latter conclusion has important implications for the design and operation of future GRB detectors, which will test the behavior of GRB number counts at intensities well below the BATSE threshold.

We have recently completed a search of 6 years of archival data from BATSE for GRBs and other transients that did *not* activate the real-time burst detection system (or "trigger") running on board the spacecraft. A GRB or other transient may fail to activate the BATSE onboard burst trigger for any of several reasons. The burst may be too faint to exceed the onboard detection threshold, it may occur while the onboard trigger is disabled for technical reasons, it may occur while the onboard trigger is optimized for detecting non-GRB phenomena, or it may artificially raise the onboard background estimate and be mistaken for a below-threshold event. Our search of the archival data is sensitive to GRBs with peak fluxes (measured over 1.024 s in the 50–300 keV energy range) that are a factor of ~ 2 lower than can be detected with the onboard trigger in its nominal configuration. Thus our search constitutes an experiment that is ~ 2 times more sensitive than those reported in the BATSE catalogs (Fishman et al. 1994; Meegan et al. 1996; Paciesas et al. 1999[7]).

In this paper we present results regarding the peak flux distribution of the GRBs detected with our "off-line" search of archival data. In § 2 we summarize some important aspects of our off-line search and discuss the $\langle V/V_{\max} \rangle$ statistic for the bursts we detected. We show that surprisingly few bursts are found on the 4.096 s and 8.192 s timescales that were not already detected on the 1.024 s timescale. In § 3 we fit parametric cosmological models to the observed differential peak flux distribution to compare scenarios in which the GRB rate follows the SFR with the model in which the comoving GRB rate is independent of redshift. We also examine the possibility that a homogeneous (in Euclidean space) population of bursting objects could be contributing to the observed sample of GRBs. In § 4 we show how our results provide two independent arguments that favor models in which the GRB rate follows the SFR over models in which the GRB rate is independent of redshift.

2. THE SEARCH FOR NONTRIGGERED GRBS

The details of our off-line search of the BATSE data are discussed in Kommers et al. (1997). We have merely extended the search from covering 345 days of the mission to covering 2200 days. We have also made minor modifications to our peak flux estimation procedure in order to secure better relative calibration between our peak fluxes and those in the 4B catalog (Paciesas et al. 1999). The extended catalog of nontriggered events will be provided and discussed in the Non-Triggered Supplement to the BATSE Gamma-Ray Burst Catalogs (Kommers et al. 2000, in preparation[8]). Here we address only those aspects of the search that are relevant to the GRB intensity distribution analysis.

We use the data from the Large Area Detectors that provide count rates in four energy channels with 1.024 s time resolution (the data type designated "DISCLA" in the flight software; Fishman et al. 1989). These data are searched for statistically significant count rate increases to identify candidate burst events. The many candidate events ("off-line triggers") are then visually inspected to separate astronomically interesting transients from instrumental and terrestrial effects. To be considered a GRB, a candidate must exhibit significant signal in the 50–300 keV range (DISCLA channels 2 and 3) and it must *lack* any characteristics that would associate it with a solar flare, Earth magnetospheric particle precipitation, or other non-GRB origin. Since the DISCLA data are (nearly) continuously recorded, our search detects some bursts that already activated the onboard burst trigger; we call these events "onboard-triggered bursts." Bursts that were detected *exclusively* by our search of archival data are called "nontriggered bursts."

In addition to searching at the 1.024 s time resolution of the DISCLA files, we also search the data binned at 4.096 s and 8.192 s time resolution. The longer time bins provide greater sensitivity to faint bursts that have durations longer than ~ 4 or ~ 8 s. The specific time profile of each burst determines which of these three timescales is the most sensitive. For this reason the searches on each timescale should be considered separate experiments.

Our search covers 1.33×10^8 s of archival data spanning the time from 1991 December 9 to 1997 December 16. In these data we detected 2265 GRBs, of which 1392 activated the onboard burst trigger and 873 did not. We will refer to these 2265 GRBs as the "off-line GRB sample." During the same time period, the onboard burst trigger detected 1815 GRBs. The $1815 - 1392 = 423$ bursts that were detected by the onboard burst trigger but that were *not* detected by our search either occurred during gaps in the archival DISCLA data or had durations much less than the 1.024 s time resolution (so they did not achieve adequate statistical significance in the archival data).

Note that because the best time resolution available to our retrospective search is 1.024 s, all results in this paper pertain to bursts with durations longer than about 1 s. Thus, the population of "short" (duration less than ~ 2 s) bursts that contributes to the bimodal GRB duration distribution (Kouveliotou et al. 1993) is not well represented in the off-line sample. An estimate for the fraction of bursts that our search is likely to miss because of our time resolution can be obtained from the 4B catalog. Although 21% of GRBs for which both durations and fluences were available had $T_{90} < 1.024$ s, only 7% had both $T_{90} < 1.024$ s and fluences

[7] Also see http://www.batse.msfc.nasa.gov/batse/grb/catalog/4b/.

[8] See http://space.mit.edu/BATSE.

too small to create adequate statistical significance in the 1.024 s data (Paciesas et al. 1999).

For each of the 873 nontriggered GRBs we have estimated a peak flux in the 50–300 keV range based on the time bin with the most counts above background. For 1288 of the 1392 onboard-triggered GRBs, we used the peak fluxes from the current BATSE GRB catalog (Paciesas et al. 1999). For the remaining 104 onboard-triggered bursts, peak fluxes were not available from the current burst catalog; we estimated peak fluxes for them using our own techniques as we did for the nontriggered bursts.

Since the onboard trigger criteria were changed for a variety of reasons during the time spanned by our search, we adopt for the nominal onboard detection threshold the value 0.3 photons cm^{-2} s^{-1} in the 50–300 keV range. At this peak flux the onboard trigger efficiency is ≈ 0.5 (Paciesas et al. 1999). With this estimate, 551 of our 873 nontriggered bursts were below the nominal onboard detection threshold. The rest were not detected on board for the reasons cited previously.

2.1. *Trigger Efficiency*

To determine the peak flux threshold of the off-line GRB sample, the trigger efficiency $E_1(P)$ of our off-line search has been calculated using the techniques described in Kommers et al. (1997). This quantity is the probability that a burst that occupies exactly one 1.024 s time bin with a peak flux P will be detected by the off-line search algorithm. $E_1(P)$ is well represented (within the uncertainties of the calculation owing to variations in the background rates) by the following function:

$$E_1(P) = \tfrac{1}{2}[1 + \mathrm{erf}\,(-3.125 + 16.677P)]\ , \qquad (1)$$

where erf (x) is the standard error function and P is given in units of photons cm^{-2} s^{-1} in the 50–300 keV band. This equation is plotted as the dashed line in Figure 1. Error bars on the grid points of the calculation (*diamonds*) represent the sample standard deviation of the calculated probabilities owing to variations in the background rates. For comparison, the BATSE trigger efficiency from the 4B catalog (Paciesas et al. 1999) is plotted as the dotted line (grid points indicated by *open squares*). Equation (1) tends to *underestimate* the probability that a typical GRB will be detected, however. This is because many GRBs in our sample last longer than 1.024 s; therefore, these bursts have more than one statistical chance to be included in the sample.

Suppose the peak of a burst occupies N time bins, so that the burst has effectively N statistical chances to be detected. Then the probability that the burst is detected can be approximated as unity minus the probability that the burst *fails* to be detected in all N trials:

$$E_N(P) = 1 - [1 - E_1(P)]^N\ . \qquad (2)$$

Since the number of chances N is not known for GRBs a priori, the actual probability of detection $E(P)$ is obtained by marginalizing $E_N(P)$ over the distribution of N for bursts with peak fluxes near P:

$$E(P) = \frac{\sum h(N, P)E_N(P)}{\sum h(N, P)}\ . \qquad (3)$$

Our estimate for $h(N, P)$, the histogram of the various integer values of N for bursts with peak fluxes near P, was obtained from the detected sample of bursts by counting, for each burst, the number of time bins with count rates that were within one standard deviation of the peak count rate. For purposes of illustration, Figure 2 shows the histogram of N for bursts with peak fluxes in the range 0.1–0.4 photons cm^{-2} s^{-1}. The resulting function $E(P)$ is well represented (to within the uncertainties of the calculation) by

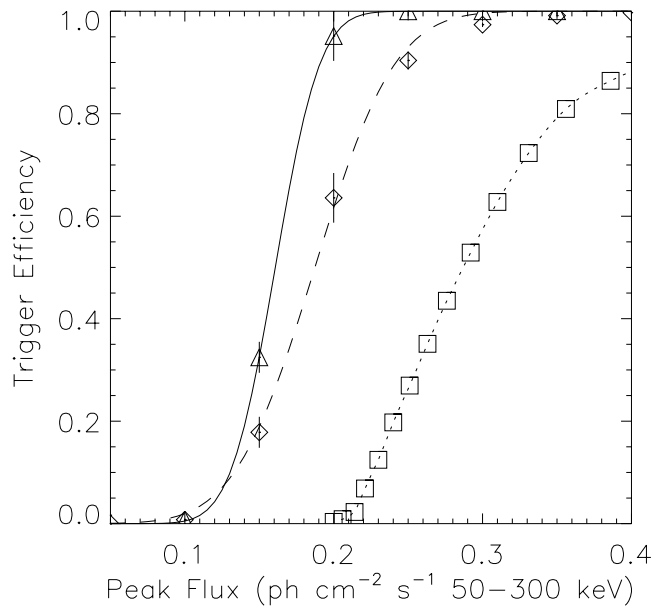

FIG. 1.—Trigger efficiency for our off-line search. The grid points of the calculations are plotted as individual symbols. Error bars represent the standard deviations of the calculated probabilities owing to variations in the background rates. The dashed line (eq. [1]) shows the probability that a burst occupying a single time bin is detected by our search. The solid line (eq. [4]) shows the marginal probability that a burst is detected by our search, given that some bursts longer than 1.024 s have more than one statistical chance to be detected. For comparison, the dotted line shows the trigger efficiency from the 4B catalog; no uncertainties are available for the grid points (*squares*).

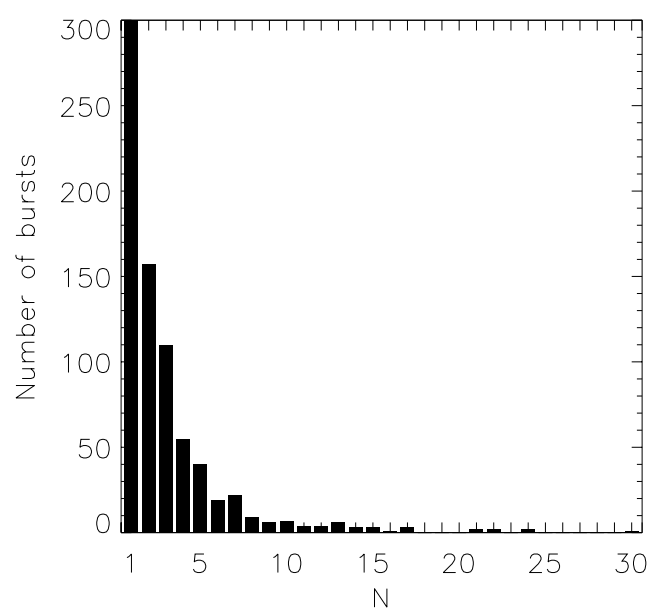

FIG. 2.—Histogram of N, the number of time bins within one standard deviation of the peak count rate, for bursts with peak fluxes in the range 0.1–0.4 photons cm^{-2} s^{-1}.

the formula

$$E(P) = \tfrac{1}{2}[1 + \mathrm{erf}\,(-4.801 + 29.868P)]\ . \qquad (4)$$

This equation expresses our best estimate of the trigger efficiency of our off-line search on the 1.024 s timescale. It is plotted as the solid line in Figure 1. The efficiency of our search falls below 0.5 at a peak flux of 0.16 photons cm^{-2} s^{-1}.

If we had not made some correction for the effect of time profiles on the single–time-bin burst detection probabilities, we would have substantially underestimated our trigger efficiency near the detection threshold ($\sim$0.2 photons cm^{-2} s^{-1}). We note that this type of correction to the single–time-bin trigger efficiency should also be applied when using the trigger efficiencies given in the 1B, 2B, 3B, and 4B catalogs (Fishman et al. 1994; Meegan et al. 1996; Paciesas et al. 1999). Similar considerations are addressed by in't Zand & Fenimore (1994) and Loredo & Wasserman (1995).

2.2. $(C_{\min}/C_{\max})^{3/2}$ *Distribution*

As successively more sensitive instruments have been used to produce GRB catalogs, it has been customary to give the value of the $\langle V/V_{\max}\rangle$ statistic for the detected bursts (Schmidt, Higdon, & Hueter 1988). For photon counting experiments like BATSE, it is not strictly $\langle V/V_{\max}\rangle$ that is typically calculated, but rather $\langle (C_{\min}/C_{\max})^{3/2}\rangle$, where $C_{\min}$ is the threshold count rate and $C_{\max}$ is the maximum count rate measured during the burst. The departure of $\langle (C_{\min}/C_{\max})^{3/2}\rangle$ from the value of $\frac{1}{2}$ expected for a population of bursters distributed homogeneously in Euclidean space (with a well-behaved, but otherwise arbitrary luminosity distribution) has been firmly established (Meegan et al. 1992, 1996). Since the discovery that most GRBs originate at cosmological distances, the quantity $\langle (C_{\min}/C_{\max})^{3/2}\rangle$ can no longer be interpreted as $\langle V/V_{\max}\rangle$. Nevertheless, it is useful to compare the values of $\langle (C_{\min}/C_{\max})^{3/2}\rangle$ obtained by successively more sensitive experiments, including the value obtained for the bursts detected with our search.

Table 1 lists various missions and the values they obtained for $\langle (C_{\min}/C_{\max})^{3/2}\rangle$. The trend toward lower values of $\langle (C_{\min}/C_{\max})^{3/2}\rangle$ with more sensitive experiments indicates that increasing the accessible survey volume by decreasing the flux threshold does not lead to the detection of large numbers of faint bursts.

The value of $\langle (C_{\min}/C_{\max})^{3/2}\rangle$ for the 2265 GRBs detected by our search[9] is 0.177 ± 0.006. *This is the lowest value ever obtained for a sample of GRBs*. The cumulative distribution of $(C_{\min}/C_{\max})^{3/2}$ for our GRBs is shown in Figure 3. The flattening of this curve in the range $0.5 < (C_{\min}/C_{\max})^{3/2} < 1.0$ shows that over 90% of the GRBs we detect are above threshold (on at least one of the three timescales) by a factor of at least $(0.5)^{-3/2} = 1.6$.

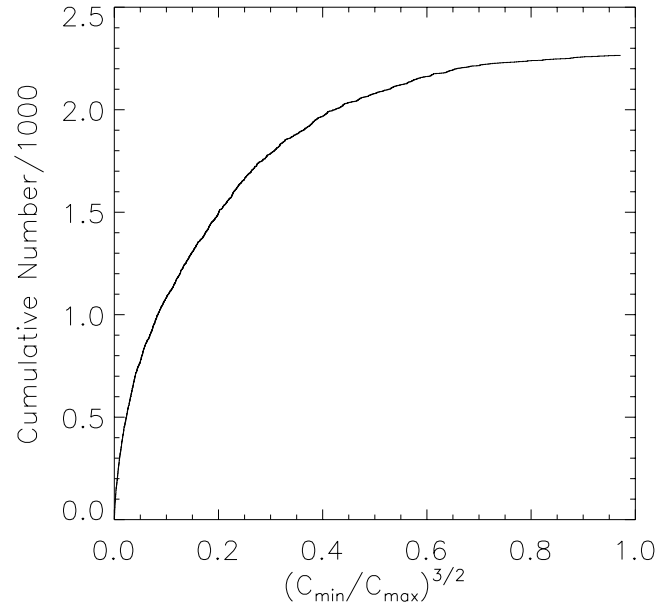

FIG. 3.—Cumulative distribution of $(C_{\min}/C_{\max})^{3/2}$ for the off-line GRB sample. The dramatic flattening of the curve above $(C_{\min}/C_{\max})^{3/2} = 0.5$ shows that few of the GRBs detected in our search are just barely above the detection threshold on all three timescales (1.024 s, 4.096 s, and 8.192 s).

The reason for this low value of $\langle (C_{\min}/C_{\max})^{3/2}\rangle$ is the fact that most of the bursts we detected had their maximum signal-to-noise ratios on the 4.096 s and 8.192 s timescales, yet surprisingly few bursts were detected *only* on these longer timescales. For each burst we compute the values of $(C_{\min}/C_{\max})^{3/2}$ on each of the three timescales. The largest of the three values for each burst is used in taking the average. In Euclidean space this corresponds to taking for each burst the *smallest* value of $\langle V/V_{\max}\rangle$. Since 72.0% of the bursts we detected have T_{90} durations (Koshut et al. 1996) longer than 8 s, we expect the average $\langle (C_{\min}/C_{\max})^{3/2}\rangle$ to be dominated by values measured on the 8.192 s timescale.

In fact, the average $\langle (C_{\min}/C_{\max})^{3/2}\rangle = 0.177 \pm 0.006$ includes 520 values measured on the 1.024 s timescale, 491 values measured on the 4.096 s timescale, and 1254 values measured on the 8.192 s timescale. Yet only 105 bursts were detected *exclusively* on either of the 4.096 or 8.192 s timescales (or both). Many of the bursts that are barely above

[9] This value supersedes the ones given in Kommers et al. (1996, 1997, 1998), which are incorrect because of a programming error. An erratum has been published (Kommers et al. 1999).

TABLE 1

VALUES OF $\langle (C_{\min}/C_{\max})^{3/2}\rangle$ OBTAINED BY VARIOUS GRB DETECTORS

Detector/Mission	$\langle (C_{\min}/C_{\max})^{3/2}\rangle$	Reference
PVO	0.46 ± 0.02	Hartmann et al. 1992
Konus/*Venera 11 and 12*	0.45 ± 0.03	Higdon & Schmidt 1990
A4/*HEAO 1*	0.40 ± 0.08	Schmidt et al. 1988
GRS/*SMM*	0.40 ± 0.025	Matz et al. 1992
GBD/*Ginga*	0.35 ± 0.035	Ogasaka et al. 1991
BATSE/*CGRO* (3B)	0.33 ± 0.01	Meegan et al. 1996
BATSE/*CGRO* (off-line,1.024 s search only)	0.247 ± 0.006	This paper
BATSE/*CGRO* (all off-line)	0.177 ± 0.006	This paper

the detection threshold on the 1.024 s timescale are well above the detection threshold on the longer timescales. Thus very few bursts are found to be just barely above our detection threshold on all three timescales, and this accounts for the low value of $\langle (C_{\min}/C_{\max})^{3/2} \rangle$. Restricting our calculation to use *only* count rates measured on the 1.024 s timescale (and bursts detected on the 1.024 s timescale) gives a larger value, $\langle (C_{\min}/C_{\max})^{3/2} \rangle = 0.247 \pm 0.006$.

Roughly, the 4.096 s search should be ~ 2 times more sensitive than the 1.024 s search for bursts that maintain their peak flux for at least ~ 4 s, and the 8.192 s search should be yet more sensitive. Therefore our lack of GRB detections exclusively on the longer timescales indicates either (1) a substantial paucity of faint, long bursts below the threshold of our 1.024 s search or (2) that during our visual inspection of the off-line triggers we have tended to classify a substantial number of faint, long GRBs as other (non-GRB) phenomena. We feel that both alternatives must be present at some level.

A review of the non-GRB off-line triggers suggests that events resembling faint, long GRBs that illuminate the same detectors as a known, bright, variable X-ray source are more likely to be attributed to variability from the X-ray source than to be classified as GRBs. There is also a tendency to classify bursts that have directions consistent with the Sun as solar flares. A secondary evaluation of the event classifications suggests that between 50 and 200 (this range represents the central 90% confidence interval), with a most likely value of 86, GRBs have been misclassified in this way. The corresponding "loss rate" is between 2% and 8% (most likely 4%) of the total 2265 bursts in the off-line sample. This is not enough to fully explain, as experimental error, the dearth of faint, long bursts below our 1.024 s threshold.

2.3. *Peak Fluxes*

Detailed comparisons of cosmological models with the data require intensity distributions in physical units. We have chosen to do the analysis in terms of the burst rate as a function of peak photon flux measured over 1.024 s in the energy range 50–300 keV. Compared with the fluence (total energy per unit area deposited in the detector by the burst), we prefer peak photon flux for the purposes of intensity analysis. The peak photon flux can be obtained more reliably from the raw count data, and it is more directly related to our ability to detect bursts.

Of the 2265 GRBs detected by our search, we chose to include in our peak flux analysis only those that were detected on the 1.024 s timescale, so that equation (4) gives the detection efficiency. We also chose to use only those bursts with peak fluxes in the range 0.18–20.0 photons $\mathrm{cm}^{-2}\ \mathrm{s}^{-1}$. The lower limit ensures that the off-line trigger efficiency exceeds 0.8 for the range of intensities used in the analysis and the upper limit excludes very bright bursts, which are too rare to provide adequate counting statistics in narrow peak flux bins. With these cuts on the data, we are left with 1998 peak flux measurements. To fit the differential intensity distribution, we bin the 1998 bursts into 25 peak flux intervals that were chosen to be approximately evenly spaced in the logarithm of P. The spacing is $\Delta \log P \approx 0.05$ in the range $0.18 < P < 1.0$, $\Delta \log P \approx 0.1$ in the range $1.0 < P < 7.9$, and there is a final broad bin for the range $7.9 < P < 20.0$. Uncertainties in the number of bursts ΔN_{obs} in each bin are taken to be $\pm(\Delta N_{\mathrm{obs}})^{1/2}$. The burst rate is computed by dividing the number of bursts in each bin by the live time of the search (1.33×10^8 s = 4.21 yr) and the mean solid angle visible to the BATSE detectors ($0.67 \times 4\pi$). Table 2 gives the peak flux intervals, number of bursts, and burst rate for each bin.

3. COSMOLOGICAL MODEL COMPARISON

Many investigators, in scores of papers, have shown the consistency of the GRB peak flux distribution with various cosmological models (see, for example, Wijers et al. 1998; Loredo & Wasserman 1998; Hakkila et al. 1996; Horack et al. 1996; Rutledge et al. 1995; Fenimore & Bloom 1995, and references therein). As shown in the previous section, the off-line GRB sample extends the observed GRB intensity distribution to peak fluxes that are lower by a factor of ~ 2 than could be studied previously. While it is unlikely that a factor of ~ 2 will yield stringent new model constraints, it remains of interest to note a few cosmological models that provide good fits to the extended GRB peak flux distribution. These can be used to set limits on the rate of GRBs that may come from a nearby, spatially homogeneous subpopulation of burst sources.

3.1. *Purely Cosmological Models*

To limit the number of free parameters that must be considered, our choice of cosmological world model is the Einstein–de Sitter model ($\Omega = 1$, $\Lambda = 0$, $q_0 = \frac{1}{2}$; Weinberg 1972). This cosmology has been used by many other investigators so it allows easy comparison of results. Where needed, we assume a Hubble constant of $H_0 = 70\ h_{70}$ km $\mathrm{s}^{-1}\ \mathrm{Mpc}^{-1}$. We also assume that bursters are distributed

TABLE 2

DATA FOR FITTING DIFFERENTIAL PEAK FLUX DISTRIBUTION

P_1	P_2	ΔN_{obs}	ΔR ($\mathrm{yr}^{-1}\ \mathrm{sr}^{-1}$)
0.180.....	0.202	87	2.45 ± 0.26
0.202.....	0.227	83	2.34 ± 0.26
0.227.....	0.254	99	2.80 ± 0.28
0.254.....	0.285	111	3.13 ± 0.30
0.285.....	0.320	92	2.60 ± 0.27
0.320.....	0.359	96	2.71 ± 0.28
0.359.....	0.403	95	2.68 ± 0.27
0.403.....	0.452	114	3.22 ± 0.30
0.452.....	0.507	93	2.62 ± 0.27
0.507.....	0.569	79	2.23 ± 0.25
0.569.....	0.639	82	2.31 ± 0.26
0.639.....	0.717	91	2.57 ± 0.27
0.717.....	0.804	73	2.06 ± 0.24
0.804.....	0.902	83	2.34 ± 0.26
0.902.....	1.000	52	1.47 ± 0.20
1.000.....	1.259	117	3.30 ± 0.31
1.259.....	1.584	111	3.13 ± 0.30
1.584.....	1.995	104	2.93 ± 0.29
1.995.....	2.511	72	2.03 ± 0.24
2.511.....	3.162	59	1.66 ± 0.22
3.162.....	3.981	48	1.35 ± 0.20
3.981.....	5.011	40	1.13 ± 0.18
5.011.....	6.309	27	0.76 ± 0.15
6.309.....	7.943	26	0.73 ± 0.14
7.943.....	20.00	64	1.80 ± 0.23

isotropically, so the only interesting parameter in the burster spatial (redshift) distribution is the radial coordinate $r(z)$ from Earth. The following derivation of the expected peak flux distributions follows the discussions in Fenimore & Bloom (1995) and Loredo & Wasserman (1997).

In general the rate of bursts R per unit interval in peak flux P observable at Earth is given by

$$\frac{dR}{dP} = \int dL \int dz \, \frac{\partial^2 R}{\partial L \, \partial z} \, \delta[(P - \Phi(L, z)] \, , \tag{5}$$

where L is the equivalent isotropic peak luminosity of the burst at the source, z is the redshift parameter, $\partial^2 R/\partial L \, \partial z$ is the rate of bursts per unit L per unit redshift interval, $\delta(x)$ is the Dirac delta function, and $\Phi(L, z)$ is the peak photon flux measured at Earth for a burst with peak luminosity L located at redshift z. We will assume that the redshift and luminosity distributions are independent, so that the burst rate as a function of L and z is given by

$$\frac{\partial^2 R}{\partial L \, \partial z} = \frac{4\pi c R_0}{H_0} \, \psi(L) \rho(z) \, \frac{r^2(z)}{(1 + z)^2 \sqrt{1 + z}} \, , \tag{6}$$

where R_0 is an overall normalization, $\psi(L)$ is the distribution of burst luminosities (normalized to unity), $\rho(z)$ is the distribution of the comoving burst rate as a function of redshift (normalized to unity on the interval $0 < z < 10$), and $r(z) = (2c/H_0)[1 + z - (1 + z)^{1/2}]/(1 + z)$ is the comoving radial coordinate.

The peak flux $\Phi(L, z)$ observed at Earth in the 50–300 keV energy range, where the BATSE burst trigger is sensitive, depends on the intrinsic spectrum of the GRB. We write it as

$$\Phi(L, z) = \frac{L K(z)}{4\pi(1 + z) r^2(z)} \, . \tag{7}$$

The spectral correction function $K(z)$ depends on the shape of the burst photon energy spectrum at the source. The observed GRBs have a variety of spectral shapes, and in the cosmological scenario these observed spectra have been redshifted according to the (unknown) redshifts of the sources.

To account for the spectral variety of GRBs we use the spectral fits of Band et al. (1993). To account for the unknown redshift factors for these spectra, we use the procedure described in Fenimore & Bloom (1995). The peak fluxes of the bursts for which Band et al. (1993) derived spectral fits are used in conjunction with the cosmological model under consideration to self-consistently estimate the redshift factors for the fitted spectra. We assume that the ith burst fitted by Band et al. (1993) has exactly the mean intrinsic peak luminosity in the cosmological model being considered: $L_i = \int dL' \, L' \psi(L')$, where the shape of $\psi(L)$ depends on the parameters of the model luminosity function. We then solve for the redshift z_i, which the fitted burst i must have had to produce the peak flux listed for it in the current BATSE GRB catalog. Fifty-one of the bursts fitted by Band et al. (1993) had peak fluxes available. For each of their spectral shapes $\phi_i(E)$ the spectral correction function takes the form

$$K_i(z) = \frac{\int_{50(1+z)/(1+z_i)}^{300(1+z)/(1+z_i)} dE \, \phi_i(E)}{(1 + z_i) \int_{30/(1+z_i)}^{2000/(1+z_i)} dE \, E \phi_i(E)} \, . \tag{8}$$

The integrals in the denominator and numerator convert the model parameter L, which represents the peak luminosity in the 30–2000 keV range at the source, to the observed photons $\mathrm{cm}^{-2} \, \mathrm{s}^{-1}$ in the 50–300 keV band at Earth. The burst rate expected in the BATSE band pass for the ith spectral shape $\phi_i(E)$ is then (from eq. [5])

$$\left(\frac{dR}{dP}\right)_i = \frac{16\pi^2 c R_0}{H_0} \int dz \, \frac{\rho(z) r^4(z)}{(1 + z)\sqrt{1 + z} K_i(z)} \times \psi\left[\frac{4\pi(1 + z) r^2(z) P}{K_i(z)}\right] . \tag{9}$$

The limits on the integral are determined by the range of z for which $\psi[4\pi(1 + z) r^2(z) P/K_i(z)]$ is nonzero at the given P.

To estimate the observed distribution of bursts, which includes a variety of spectral shapes, we average equation (9) over the 51 spectral correction functions $K_i(z)$. This procedure is equivalent to marginalizing the unknown spectral parameters of the observed bursts (i.e., those in the off-line sample) to obtain the posterior rate distribution. The 51 spectra from Band et al. (1993) are furnishing estimates of the prior distributions of the spectral parameters. The expectation value of the observed burst rate for peak fluxes between P_1 and P_2 is then

$$\Delta R(P_1, P_2) = \int_{P_1}^{P_2} dP \, E(P) \left\langle \frac{dR}{dP} \right\rangle , \tag{10}$$

where $\langle dR/dP \rangle$ is the mean rate estimated from the 51 observed spectra and $E(P)$ is the detection efficiency.

The use of the Band et al. spectra increases the computational cost of the rate model by a factor of ~ 50 over using a single "universal" burst spectrum. We found that a simple power-law form for the GRB photon energy spectrum—as has been used by many previous studies—predicts significantly different burst rates at low peak fluxes than does equation (10). Since we are interested in the behavior of the burst rate at low peak fluxes, we felt that the analysis based on the full 51 Band et al. spectra would be more reliable. Similar conclusions are reached by Fenimore & Bloom (1995) and Mallozzi, Pendleton, & Paciesas (1996).

For comparison with the results of previous studies, we chose two forms for the luminosity distribution. The first is a monoluminous (standard candle) distribution. The second is a truncated power law,

$$\psi(L) = \begin{cases} \dfrac{1}{L \log (L_{\max}/L_{\min})} \, , & \beta = 1 \, , \\ \dfrac{(1 - \beta) L^{-\beta}}{L_{\min}^{1-\beta} - L_{\max}^{1-\beta}} \, , & \beta \neq 1 \, , \end{cases} \tag{11}$$

with $\psi(L) = 0$ if $L < L_{\min}$ or $L > L_{\max}$. The normalization factors ensure that $\int dL \, \psi(L) = 1$.

The standard candle distribution, though useful for comparison with other results, is ruled out by the observed peak fluxes of the four bursts for which associated optical redshifts have been measured. For GRBs 970508, 971214, 980613, and 980703 the inferred equivalent isotropic peak luminosities in the 30–2000 keV energy range are given in Table 3. To calculate each of these peak luminosities, we have used the observed 50–300 keV peak flux (on the 1.024 s timescale) in combination with the observed redshift to find the expectation value of the intrinsic luminosity averaged over the 51 Band et al. spectra. This procedure is the one

TABLE 3

REDSHIFTS AND IMPLIED EQUIVALENT ISOTROPIC PEAK LUMINOSITIES

GRB	Peak Flux (50–300 keV)	z	Implied L (10^{51} h_{70}^{-2} ergs s^{-1} in 30–2000 keV)
970508.....	0.97 ± 0.05	0.835[a]	0.6 ± 0.1
971214.....	1.95 ± 0.05	3.418[b]	37 ± 16
980613.....	0.63 ± 0.05[c]	1.096[d]	0.8 ± 0.2
980703.....	2.39 ± 0.06	0.966[e]	2.2 ± 0.4

[a] Metzger et al. 1997.
[b] Kulkarni et al. 1998a.
[c] Woods, Kippen, & Connaughton 1999.
[d] Djorgovski et al. 1999.
[e] Djorgovski et al. 1998.

used in our modeling, so it was used on these four bursts also, to facilitate comparisons with the models (see § 4). The peak luminosities estimated here are somewhat higher by factors of ~3 to ~6 than those reported elsewhere (e.g., Krumholz et al. 1998). This is because the spectral shapes fitted by Band et al. (1993) generally become steeper at high energies, so a source at high redshift must be more luminous to produce the flux observed at Earth than it would have to be if the spectrum did not fall off so rapidly at higher energies. These differences illustrate the importance of using the most realistic spectral models available rather than simple power laws when analyzing the GRB intensity distribution.

A variety of spatial, or rather redshift, distributions for the bursters have been used in previous studies of the GRB intensity distribution. With up to four free parameters already incorporated into our burst rate models (the overall normalization R_0, and the parameters of the power-law luminosity function β, $L_{\min}$ and $L_{\max}$) there is little hope of constraining any additional free parameters in the redshift distribution. Here we explore three specific models of the redshift distribution that contain no free parameters. The two physical scenarios we examine are (1) that the comoving burst rate is independent of redshift between $z = 0$ and $z = 10$ and (2) that the comoving GRB rate is proportional to the star formation rate (SFR).

For the GRB rate model that is independent of redshift, $\rho(z) = 0.1$ for $0 < z \leq 10$ and $\rho(z) = 0$ for $z > 10$. We refer to this redshift distribution as "model D1."

For the case where the burst rate follows the star formation history of the universe, we use two slightly different parameterizations of the SFR. The first is the SFR deduced from the rest-frame ultraviolet luminosity density, with the functional form given in footnote 1 of Madau, Della Valle, & Panagia (1998a). In this estimation the SFR peaks around $z = 1$–1.5. A SFR of roughly this form has been used by several previous studies of the GRB intensity distribution (Totani 1997; Wijers et al. 1998; Krumholz et al. 1998). We refer to this redshift distribution as "model D2."

The second SFR parameterization assumes that the SFR—and thus the GRB rate—tracks the total output of radio-loud active galactic nuclei (AGNs). In this scenario the SFR peaks at $z = 2$–3 (Hughes et al. 1998; Dunlop 1998). This form of the SFR appears to be more consistent with recent results from SCUBA (Hughes et al. 1998), which are not susceptible to the same problems of dust obscuration as the determination by Madau et al. (1998a, 1998b). The specific functional form we use is a best-fit analytic model to points measured by hand from Figure 6 of Hughes et al. (1998): $\rho(z) \propto 0.00360 + 0.0108 \exp(2.76z - 0.573z^2)$. This approximation appears to be accurate to within 5% for the redshift range $1 < z < 4$. (At lower and higher redshifts the formula likely underestimates the actual rate of star formation, but this is no great concern as it is the redshift of the peak SFR that is of primary interest.) We refer to this redshift distribution as "model D3."

With choices for $\psi(L)$ and $\rho(z)$ as discussed, we fit equation (10) to the data in Table 2 by minimizing the χ^2 statistic. In all cases, we found that the parameter $L_{\max}$ was not well constrained: variations in $L_{\max}$ did not change the minimum χ^2 by a significant amount. The (mathematical) reason for this is that the integrand in equation (9) is a decreasing function of z for plausible values of β, so that varying the upper limit ($z_{\max}$ corresponding to $L_{\max}$ for the given P) causes only small changes in the value of the integral. Accordingly, all the results reported here set $L_{\max} \equiv 1000L_{\min}$. The free parameters are thus R_0 and L_0 in the cases of the standard candle models and R_0, β, and $L_{\min}$ in the cases of the power-law luminosity distribution models. The results of the fits are listed in Tables 4 and 5. Uncertainties on the fitted parameters correspond to 68% confidence limits for two ($\Delta\chi^2 = 2.3$) or three ($\Delta\chi^2 = 3.5$) interesting parameters, respectively (Avni 1976).

Model D1 (constant burst rate density as a function of redshift) produces an acceptable fit for the standard candle luminosity distribution. The probability of getting $\chi^2 > 32.3$ for 23 degrees of freedom is 0.094. Adding one more free parameter (β) for the power-law luminosity distribution produces an insignificant change in the minimum χ^2. Furthermore, the high value of β in the best-fit power-law distribution indicates a very narrow range of peak luminosities.

Model D2 (burst rate density follows the SFR as determined by Madau et al. 1998a, 1998b) produces a formally unacceptable fit in the monoluminous case. But it achieves an excellent fit (χ^2 dof$^{-1} = 0.81$) for the power-law luminosity distribution. The F-test estimates a probability of 1.5×10^{-7} that the improvement in χ^2 is due to chance, justifying the inclusion of the additional parameter in the power-law luminosity function model. The value of β in this

TABLE 4

BEST-FIT PARAMETERS FOR MONOLUMINOUS COSMOLOGICAL MODELS

$\rho(z)$	R_0 (h_{70}^3 Gpc^{-3} yr^{-1} sr^{-1})	L_0 (10^{51} h_{70}^{-2} ergs s^{-1})	χ^2 (23 d.o.f)
D1 (constant).....	$9.45^{+0.39}_{-0.78}$	$0.40^{+0.06}_{-0.02}$	32.3
D2 (SFR)	2.0 ± 0.1	1.5 ± 0.1	64.1
D3 (AGN)	1.9 ± 0.1	$3.1^{+0.4}_{-0.2}$	27.8

TABLE 5

BEST-FIT PARAMETERS FOR COSMOLOGICAL MODELS WITH POWER-LAW LUMINOSITY FUNCTIONS

$\rho(z)$	R_0 (h_{70}^3 Gpc^{-3} yr^{-1} sr^{-1})	$L_{\min}$ (10^{51} h_{70}^{-2} ergs s^{-1})	β	χ^2 (22 d.o.f)
D1 (constant).....	8.8 ± 1.3	$0.29^{+0.08}_{-0.06}$	$4.6_{-1.4}$[a]	32.9
D2 (SFR)	2.2 ± 0.3	$0.48^{+0.20}_{-0.10}$	$2.1^{+0.3}_{-0.2}$	17.9
D3 (AGN)	2.1 ± 0.2	$1.44^{+0.53}_{-0.40}$	$2.6^{+1.0}_{-0.4}$	17.4

[a] This parameter is not constrained above the the best-fit value when the other parameters are free to vary.

model is remarkably well constrained. If the other fit parameters are regarded as "uninteresting," then the 90% ($\Delta\chi^2 = 2.7$) and 99% ($\Delta\chi^2 = 6.6$) confidence intervals (Avni 1976) on β are 2.0–2.3 and 1.8–2.6, respectively.

Model D3 (burst rate density follows the output of radio-loud AGNs) produces formally acceptable fits with both the standard candle and power-law luminosity distributions. The power-law luminosity distribution achieves a significantly lower χ^2, however. The F-test estimate of the probability that the improvement is due to chance is 1.5×10^{-3}.

Figure 4 plots the differential peak flux distributions for the best-fit models with power-law luminosity distributions. For all three best-fit models the value of $\langle (P_{\min}/P)^{3/2} \rangle$ is consistent with the value of $\langle (C_{\min}/C_{\max})^{3/2} \rangle$ measured for the sample (see § 2.2). Extrapolating the best-fit models to peak fluxes lower than those included in our data shows very different behaviors. Model D1 (*dot-dashed lines*) predicts a dramatically higher burst rate at low peak fluxes than do models D2 (*solid line*) and D3 (*dashed line*).

In each model the best-fit parameters for the power-law luminosity function yield our best estimate of the parameters of the *intrinsic* distribution of GRB peak luminosities. The distribution of peak luminosities of the *observed* bursts is different, however, because the most luminous bursts are sampled from a much larger volume than are the least luminous bursts. Even though high-luminosity bursts are infrequent, the geometrical advantage of sampling them from a larger volume means that they will be overrepresented in a sample of bursts observed over a fixed time interval. The distribution of peak luminosities for the observed bursts is the "effective luminosity function" (see Loredo & Wasserman 1997 for further discussion). For the best-fit parameters of model D1 the effective luminosity function is a power law that is less steep than that of the intrinsic luminosity function. We find $\beta_{\rm eff}^{\rm D1} = 2.8$ for the effective luminosity function versus $\beta = 4.6$ for the intrinsic one. The power-law slopes of the effective luminosity functions for models D2 and D3 are $\beta_{\rm eff}^{\rm D2} = 1.6$ and $\beta_{\rm eff}^{\rm D3} = 1.9$, respectively.

Similarly, the distribution of the GRB rate as a function of redshift for the observed bursts is not identical to the intrinsic redshift distribution given by $\rho(z)$ (see Loredo & Wasserman 1997). Figure 5 shows the effective redshift distributions for the best-fit models D1, D2, and D3. In all 3

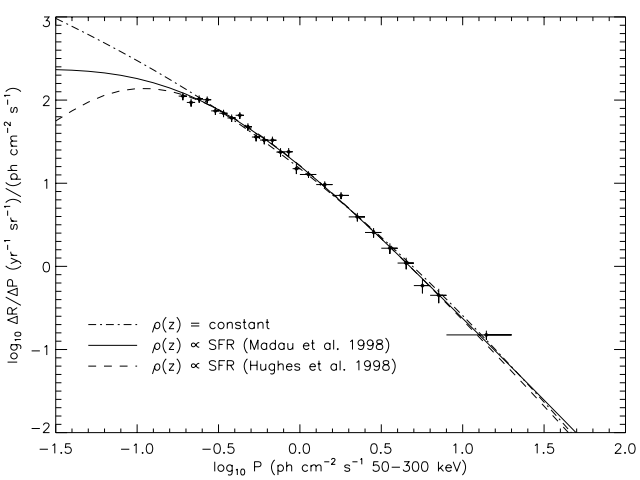

FIG. 4.—Best-fit cosmological models with power-law luminosity distributions. Units of R are bursts yr^{-1} sr^{-1}, and those of P are photons cm^{-2} s^{-1} in 50–300 keV. The dot-dashed line corresponds to model D1 (comoving burst rate is independent of redshift). The solid line shows model D2 (burst rate follows the rest-frame ultraviolet luminosity density), and the dashed line shows model D3 (burst rate follows the output of radio-loud AGNs). Measured rates are shown with 1σ vertical error bars; horizontal error bars indicate the bin widths. The best-fit model curves displayed here have not been corrected for detection efficiency.

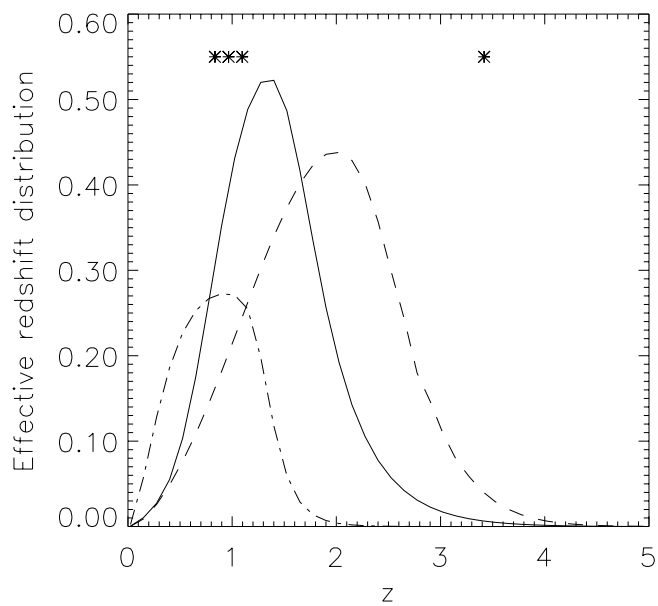

FIG. 5.—Redshift distribution of the burst rate for observed bursts (i.e., the effective differential burst rate as function of redshift). The distributions are normalized so that the integral of the distribution visible to a "perfect" detector with no sensitivity limit is unity. The dot-dashed line corresponds to a constant burst rate as a function of redshift (model D1). The solid line corresponds to the model (D2) in which the burst rate traces the SFR as determined by Madau et al. (1998a, 1998b). The dashed line corresponds to the model (D3) in which the burst rate traces the output of radio-loud AGNs (Hughes et al. 1998). In model D1 the off-line search detects a smaller percentage of the bursts that occur than it does in models D2 and D3. The redshifts associated with GRBs 970508, 971214, 980613, and 980703 are marked with asterisks.

models the effective redshift distribution cuts off at a lower redshift than does the corresponding intrinsic redshift distribution. The mean redshifts of the observed bursts in the best-fit models D1, D2, and D3 are $\langle z \rangle^{D1} = 0.86$, $\langle z \rangle^{D2} = 1.4$, and $\langle z \rangle^{D3} = 1.9$, respectively. The maximum redshifts of the bursts in models D1, D2, and D3 are not precisely determined, but the observed redshift distributions are cut off around $z_{max}^{D1} \approx 1.5$, $z_{max}^{D2} \approx 2$, and $z_{max}^{D3} \approx 3$, respectively (see Fig. 5).

It is interesting to compare the rate of bursts that are seen with the off-line search to the total rate of bursts that occur in the universe, subject to the cosmological rate models we are considering. The fraction of bursts that are detected with BATSE is given by the integral of the effective redshift distribution for the off-line search (over the range $0 < z < 10$) divided by the integral of the effective redshift distribution that would be visible to a "perfect detector," which can detect infinitely faint bursts, multiplied by the live-time (0.70) and sky exposure (0.67) fractions. In the best-fit models D1, D2, and D3, it follows that the off-line search detects $\sim 14\%$, $\sim 30\%$, and $\sim 37\%$, respectively, of the bursts that occur in the universe. Of course, these estimates can apply only to bursts with energy spectra and durations of the kind that are accessible to the off-line search. If BATSE had 100% live time and no Earth blockage, then in model D1 30% of the bursts that occur could be detected with the off-line search. In models D2 and D3, 65% and 78%, respectively, of the bursts that occur could be detected with the off-line search.

It is customary to quote the rate of GRBs as the comoving rate per unit volume at $z = 0$, a quantity often denoted by ρ_0 with units of $\mathrm{Gpc}^{-3}\ \mathrm{yr}^{-1}$ (Fenimore & Bloom 1995; Wijers et al. 1998). The model parameter R_0 is related to ρ_0 by $\rho_0 = 4\pi R_0\, \rho(0)$. Table 6 lists the values of ρ_0 corresponding to the best-fit values of R_0 for the standard-candle GRB models. Table 7 does the same for the GRB models with a power-law luminosity function. This burst rate can be converted into an event rate per "typical" galaxy using the space density of such galaxies. Here, a "typical" galaxy is taken to be one with a luminosity L^* equal to the characteristic luminosity of galaxies in the Schechter function (Schechter 1976). Loveday et al. (1992) report the mean space density of L^* galaxies to be $(4.8 \pm 0.6) \times 10^{-3}\ h_{70}^3\ \mathrm{Mpc}^{-3}$. With this conversion, the comoving rate of GRBs at $z = 0$ can be expressed in GEM (galactic events per million years), which is the rate of GRBs in an L^* galaxy. This quantity is also listed in Tables 6 and 7.

TABLE 6

COMOVING $z = 0$ BURST RATE FOR MONOLUMINOUS COSMOLOGICAL MODELS

$\rho(z)$	ρ_0 ($h_{70}^3\ \mathrm{Gpc}^{-3}\ \mathrm{yr}^{-1}$)	GEM[a] (Myr^{-1})
D1 (constant).....	$11.9^{+0.5}_{-1.0}$	~ 2
D2 (SFR)	0.78 ± 0.04	~ 0.2
D3 (AGN)	0.46 ± 0.02	~ 0.1

[a] Galactic events per 10^6 yr.

TABLE 7

COMOVING $z = 0$ BURST RATE FOR COSMOLOGICAL MODELS WITH POWER-LAW LUMINOSITY FUNCTIONS

$\rho(z)$	ρ_0 ($h_{70}^3\ \mathrm{Gpc}^{-3}\ \mathrm{yr}^{-1}$)	GEM[a] (Myr^{-1})
D1 (constant).....	11.1 ± 1.6	~ 2
D2 (SFR)	0.87 ± 0.12	~ 0.2
D3 (AGN)	0.51 ± 0.05	~ 0.1

[a] Galactic events per 10^6 yr.

3.2. *Limits on a Possible Homogeneous Subpopulation*

The discovery of the unusual Type Ib/c supernova SN 1998bw in the X-ray error box of GRB 980425 has fueled speculation that the supernova (SN) produced the GRB (Galama et al. 1998; Iwamoto et al. 1998; Kulkarni et al. 1998b). It has been suggested that such events (the supernova-GRBs, or "S-GRBs") may constitute a subclass of all GRBs (Bloom et al. 1998). In this subsection we discuss what fraction of all GRBs could belong to such a subclass assuming that the remaining bursts come from the "reasonable" cosmological scenarios discussed previously.

If the inferred peak luminosity of GRB 980425 (assuming a distance corresponding to the redshift $z = 0.0085$ of SN 1998bw; Tinney et al. 1998) is typical of S-GRBs, then the bursts in this subclass are detectable within a volume of radius ~ 100 Mpc (Bloom et al. 1998). Within this volume, we assume the spatial distribution of Type Ib/c SNe to be approximately homogeneous. Thus the cumulative intensity distribution of S-GRBs can be expected to follow a $-3/2$ power law. This conclusion follows for any well-behaved distribution of intrinsic luminosities as long the spatial distribution does not deviate from homogeneity within the volume sampled by our detectors. Since the observed intensity distribution of all GRBs deviates strongly from the $-3/2$ power law, it can be used to set an upper limit on the fraction of all GRBs that can come from a subclass that obeys the $-3/2$ power law. In this respect, the faint end of the peak flux distribution (as explored by our off-line search) provides the most stringent constraints.

A model-independent limit on the fraction of bursts that might come from a nearby homogeneous population can be obtained from the histogram of $(C_{min}/C_{max})^{3/2}$ for the observed bursts. Any homogeneous subpopulation is expected to contribute a constant number of bursts to each bin in the histogram. Thus the bin with the fewest number of bursts sets an upper limit on the total number of bursts that could come from the subpopulation. The bursts detected with our search have already been used to set an upper limit of 5%–6% on the fraction of bursts that could come from a homogeneous subpopulation; this limit is therefore an upper limit on the fraction of bursts that could be associated with nearby Type Ib/c SNe (Kippen et al. 1998). Though model independent, this limit depends on how coarsely the histogram is binned. It also assumes than an arbitrary distribution of intensities is acceptable for bursts that do *not* come from the homogeneous subpopulation. This is too much freedom, because physically plausible distributions occupy only a subset of all arbitrary intensity distributions.

Here we assume that the bulk of GRBs come from the cosmological distributions discussed in § 3.1. An upper limit on the rate of all GRBs that might come from Type Ib/c SNe (or any nearby homogeneous distribution) is then fixed by determining the maximum rate of bursts that can come from a (differential) distribution proportional to $P^{-5/2}$ before the model becomes inconsistent with the data. We

TABLE 8

UPPER LIMITS ON FRACTIONAL GRB RATE (%) DUE TO A POSSIBLE HOMOGENEOUS (IN EUCLIDEAN SPACE) SUBPOPULATION OF GRBS

$\rho(z)$	90% Confidence	99% Confidence
D1 (constant).....	5.1	6.2
D2 (SFR)	6.9	10.0
D3 (AGN)	7.7	11.2

thus fit a model of the form

$$\Delta R(P_1, P_2) = R_H \int_{P_1}^{P_2} dP\, E(P) P^{-5/2} + \int_{P_1}^{P_2} dP\, E(P) \left\langle \frac{dR}{dP} \right\rangle . \quad (12)$$

The fractional burst rates corresponding to the 90% and 99% confidence upper limits on the normalization R_H in each model are given in Table 8. The upper limits were determined by finding the value of R_H for which $\Delta\chi^2 = 2.7$ and $\Delta\chi^2 = 6.6$, respectively, when χ^2 is minimized with respect to the other fit parameters (Avni 1976). In all cases, only a modest fraction, 5%–10%, of the observed GRBs could come from a homogeneous subpopulation (and thus from nearby SNe). These upper limits are comparable to the model-independent result found in the previous paragraph. They are slightly less constraining because of the fact that our peak flux distribution refers only to the 1.024 s timescale, so it takes no account of the paucity of faint bursts found on the 4.096 and 8.192 s timescales (see § 2.2).

These results were to be expected from the facts that (1) models D1, D2, and D3 with power-law luminosity distributions already gave excellent fits to the data without the presence of the homogeneous ($P^{-5/2}$) term, which is sharply peaked at low peak fluxes, and (2) the fractional uncertainties on the rates in each bin are on the order of 10%. The upper limits discussed here would be further reduced if a given GRB must exhibit certain characteristics (e.g., single-peaked time profile, lack of emission above 300 keV) in order to be considered a candidate S-GRB (Bloom et al. 1998). Norris, Bonnell, & Watanabe (1998) have found that only 0.25%–0.5% of BATSE GRBs have temporal and spectral characteristics similar to GRB 980425.

4. DISCUSSION

The GRB peak flux distribution alone (on the 1.024 s timescale) only weakly distinguishes between the nonevolving model $\rho(z) = \text{constant}$ (D1) and the evolving models, where $\rho(z)$ is proportional to an estimate of the star formation history (D2 and D3). (In this section we restrict our attention to models that include a power-law distribution of intrinsic peak luminosities.) A similar conclusion has been reached previously by Krumholz et al. (1998), who analyze the BATSE catalog data and find that to reliably distinguish the nonevolving and evolving models requires data from more sensitive GRB detectors and/or the measurement of more individual GRB redshifts.

The off-line sample of GRBs constitutes a more sensitive experiment than the one analyzed by Krumholz et al. (1998). Here we argue that models similar (or identical) to D2 and D3, in which the GRB rate has a significant peak in the redshift range $1 < z < 3$, *are modestly preferred over the constant rate density model.* Two independent lines of reasoning serve to denigrate the $\rho(z) = \text{constant}$ ("nonevolving") models in favor of the evolving ones.

First, our search on the 1.024 s timescale can reach peak fluxes as low as 0.16 photons cm^{-2} s^{-1} in the 50–300 keV band (50% detection efficiency). However, our searches on the 4.096 and 8.192 s timescales are sensitive to peak fluxes (averaged over the matching timescale) that are lower by factors of ~ 2 and $\sim 2\sqrt{2}$, respectively, than the 1.024 s threshold. In fact, most of the bursts we detect have their highest signal-to-noise ratio in the 8.192 s search. Yet surprisingly few bursts are detected *exclusively* on the longer 4.096 s and 8.192 s timescales. This suggests that there are relatively few faint GRBs waiting to be detected by a search that is more sensitive than the one we carried out. In this respect, the evolving models (D2 and D3) appear to be more accurate. They predict that the number of bursts per logarithmic peak flux interval will level off toward lower peak fluxes, and may even start to decline (see Fig. 4). The nonevolving model, on the other hand, predicts that the number of bursts observed per logarithmic peak flux interval will continue to increase toward lower peak fluxes.

Since we have not derived peak fluxes on the 4.096 and 8.192 s timescales in order to repeat the analysis of § 3.1, we offer the following quantitative evidence that the paucity of bursts detected on the longer timescales favors the evolving models D2 and D3 over the nonevolving model D1. On the 1.024 s timescale, the measured value of $\langle (C_{\min}/C_{\max})^{3/2} \rangle = 0.247 \pm 0.006$ is trivially consistent with the values of $\langle (P_{\min}/P)^{3/2} \rangle$ found for the best-fit models in § 3.1. However, the value of $\langle (C_{\min}/C_{\max})^{3/2} \rangle = 0.177 \pm 0.006$ found for *all* bursts detected by our search contains information on the paucity of faint bursts on the 4.096 and 8.192 s timescales. We can compare it with the value of $\langle (P_{\min}/P)^{3/2} \rangle$ obtained by extrapolating the best-fit models of § 3.1 to the peak flux threshold associated with the 8.192 s search. Taking $0.18/(2\sqrt{2}) = 0.06$ photons cm^{-2} s^{-1} as the approximate $P_{\min}$ for the 8.192 s search, we obtain the following values for $\langle (P_{\min}/P)^{3/2} \rangle$: 0.221 in model D1, 0.169 in model D2, and 0.147 in model D3. Thus model D2 produces a value of $\langle (P_{\min}/P)^{3/2} \rangle$ that is the most consistent with the value of $\langle (C_{\min}/C_{\max})^{3/2} \rangle$ found for our full sample, and model D1 produces the most inconsistent value.

Second, the inferred equivalent isotropic peak luminosities (in the 30–2000 keV range) of the three bursts for which associated redshifts have been measured can be compared with the effective luminosity distributions of the best-fit models. The best-fit nonevolving model (D1) predicts that 90% of all GRBs should come from the narrow range of intrinsic peak luminosities $(0.29\text{–}0.66) \times 10^{51}\ h_{70}^{-2}$ ergs s^{-1} (a factor of ~ 2). The range from which 90% of the *observed* GRBs in this model are drawn is somewhat broader, however: $(0.29\text{–}1.5) \times 10^{51}\ h_{70}^{-2}$ ergs s^{-1} (a factor of ~ 5). In contrast, the intrinsic luminosities inferred from the three bursts with associated redshift information span a much broader peak luminosity range, $(0.6\text{–}37) \times 10^{51}\ h_{70}^{-2}$ ergs s^{-1} (a factor of ~ 62). Bursts with peak luminosities as high as those inferred for GRB 971214 [$(37 \pm 16) \times 10^{51}\ h_{70}^{-2}$ ergs s^{-1}] and GRB 980703 [$(2.2 \pm 0.4) \times 10^{51}\ h_{70}^{-2}$ ergs s^{-1}] are extremely rare events if the (nonevolving) model D1 is correct. On the other hand, the best-fit (evolving) models D2 and D3 allow a much broader (and

uniformly higher) range of luminosities. The best-fit model D2 predicts that 90% of all GRBs are drawn from the intrinsic peak luminosity range (0.50–7.3) $\times 10^{51}\ h_{70}^{-2}$ ergs s^{-1} (a factor of $\sim$15) and that 90% of the observed GRBs are drawn from the range (0.53–72) $\times 10^{51}\ h_{70}^{-2}$ ergs s^{-1} (a factor of $\sim$130). Likewise, the best-fit model D3 predicts that 90% of all GRBs are drawn from the range (1.5–9.3) $\times 10^{51}\ h_{70}^{-2}$ ergs s^{-1} (a factor of $\sim$6) and 90% of the observed GRBs are drawn from the range (1.5–40) $\times 10^{51}\ h_{70}^{-2}$ ergs s^{-1} (a factor of $\sim$25). In the context of models D2 and D3, the GRBs 970508, 971214, 980613, and 980703 constitute a much more likely sample of detected bursts than in model D1.

The effective redshift distributions (the rates of observed bursts as a function of redshift) furnish another point of comparison with GRBs 970508, 971214, 980613, 980703. As shown in Figure 5 the model D1 predicts a vanishingly small rate of observed bursts from the redshift $z = 3.418$ measured for GRB 981214 (Kulkarni et al. 1998a). If model D1 were correct, then it would be remarkable that BATSE and *BeppoSAX* detected such a rare burst: only 1×10^{-6} of the rate distribution comes from higher redshifts. On the other hand, the evolving models D2 and D3 predict much higher rates of observed bursts from $z = 3.418$. Even in these models, however, such a high redshift is exceptional: in model D2 only 0.4% of the burst rate distribution lies beyond $z = 3.4$, and in model D3 only 1.8% does. Still, as in the case of the inferred luminosity distributions, the three bursts with associated redshifts are a much more likely sample in models D2 and D3, where the GRB rate follows an estimate of the star formation history.

These results certainly do not prove that the GRB rate traces the star formation rate. The peak flux distributions alone fail to exclude the nonevolving rate density model (D1) with high confidence, especially in view of the unknown cosmological parameters that can be varied to improve the fit. Furthermore, until many more redshifts are associated with specific GRBs and/or more sensitive GRB detectors go on-line, the data will not be able to distinguish qualitatively similar SFR evolution models such as D2 and D3. Any evolution that specifies a significant peak in the burst rate in the redshift range $1 < z < 3$ is likely to be consistent with current data. The reasoning regarding the paucity of faint bursts detected *only* on the 4 and 8 s timescales should be addressed more quantitatively in the context of the models, but this is difficult owing to our poor understanding of the diverse time profiles of GRBs and of the correlations between time profiles and peak fluxes. Finally, we have considered only three very specific "strawman" models, and it may be that none of them are particularly accurate representations of the true GRB rate density and peak luminosity distributions. For example, a previous episode of star formation at high redshift could contribute a hitherto undetected population of very faint GRBs.

Nevertheless, the results of our search appear to support the conclusions reached by Totani (1997), Wijers et al. (1998) and Krumholz et al. (1998), who showed that if the GRB rate traces the SFR then relatively few faint "classical" GRBs are to be found below the BATSE onboard detection threshold. This information should be useful to the designers and operators of future GRB detectors.

In Figure 6 we plot the cumulative rate distribution of the off-line sample of GRBs along with the best-fit models and

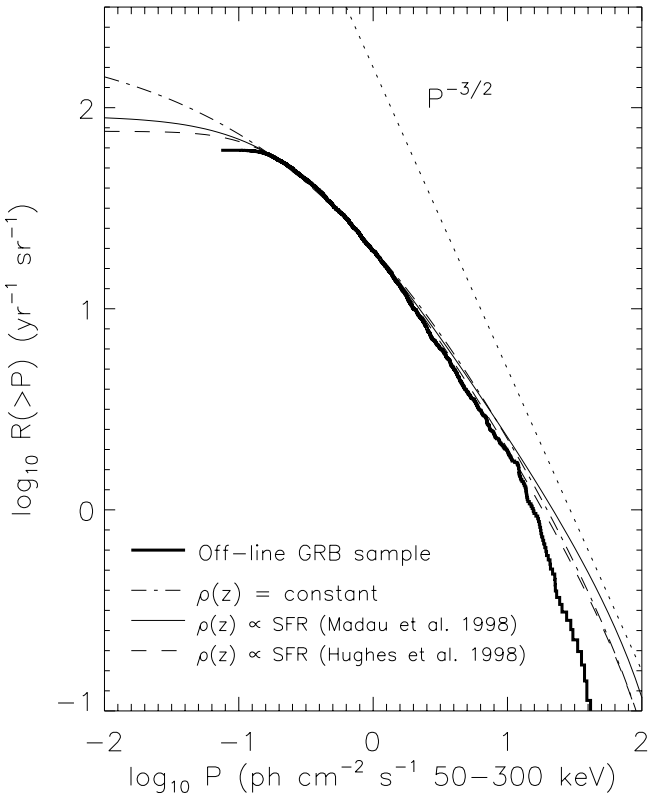

FIG. 6.—Cumulative peak flux distributions for best-fit models. The units of R are bursts $yr^{-1}\ sr^{-1}$. The observed peak flux distribution for the off-line sample is shown as the solid histogram. The best-fit model D1 is shown as the dot-dashed line. Model D2 is shown as the solid line. Model D3 is shown as the dashed line. The discrepancy at high peak fluxes is not surprising because the fitting used only data from the interval 0.18–20.0 photons $cm^{-2}\ s^{-1}$, but the curves in the figure are intended to reflect true cumulative distributions (with no lower or upper limit on peak flux). The best-fit models appear to predict too many bright bursts, though the discrepancy between the data and the models is not statistically significant unless the comparison is restricted to bright bursts only (data above 10.0 photons $cm^{-2}\ s^{-1}$). This suggests that the off-line sample should be combined with data from longer missions such as *PVO* and/or *Ulysses* to check the behavior of the burst rate at high peak fluxes.

their extrapolations to lower and higher peak fluxes than are available in the data. The best-fit models apparently predict too many bright bursts above the maximum peak flux that was used to fit the differential burst rate (20.0 photons $cm^{-2}\ s^{-1}$). This discrepancy is not surprising because the fits did not include data at high peak fluxes. A Kolmogorov-Smirnov (K-S) test (Press et al. 1995) indicates that the discrepancy is not significant if the data and best-fit models are compared for *all* peak fluxes above 0.18 photons $cm^{-2}\ s^{-1}$. (The probability of getting a larger value of the K-S statistic is 0.4 for model D2.) If the K-S test is restricted to the data above 10.0 photons $cm^{-2}\ s^{-1}$, however, the discrepancy is significant (the probability of getting a larger value of the K-S statistic is 6×10^{-4} for model D2). This means that the extrapolations of the best-fit models are inaccurate at high peak fluxes.

Future research should explore the peak flux distribution over the widest possible range. For example, the GRB detector on board *Pioneer Venus Orbiter* (*PVO*) operated for a much longer mission than has BATSE (so far) and it has more completely sampled the rate of very bright bursts.

When the peak fluxes of the GRBs detected with *PVO* are calibrated to match the BATSE peak fluxes, it would be of interest to see if the parameters of the best-fit models found in this paper remain consistent with the number counts when the very bright bursts are included. Figure 6 shows that the slopes of the best-fit models approach the $-\frac{3}{2}$ slope reported to be consistent with the brightest *PVO* bursts (Fenimore et al. 1993).

The results of the best-fit models are otherwise generally consistent with previous studies of the BATSE data. In particular we find that while we cannot constrain the full width of the power-law luminosity function in any of the scenarios we considered, the best-fit models yield intrinsic peak luminosity functions that contain 90% of all GRBs within a factor of 10–20. This result (or a similar one) has been previously obtained by Ulmer, Wijers, & Fenimore (1995), Woods & Loeb (1995), Hakkila et al. (1996), and Horack et al. (1996). We find that the peak luminosity distribution of the observed bursts, however, is wider: in model D2, 90% of the observed bursts come from a peak luminosity range that spans a factor of ~ 100 or more. A similar result is discussed by Loredo & Wasserman (1998).

The effective redshift distributions that we obtain (see Fig. 5) are reasonably consistent with those obtained by Krumholz et al. (1998) and Mao & Mo (1998) using the BATSE catalog data. They are also consistent with limits on the redshifts of GRB sources set by the nondetection of any gravitationally lensed GRBs in the BATSE catalogs (Marani et al. 1998). Holz, Miller, & Quashnock (1998) derive upper limits of $\langle z \rangle = 2.3$ (68% confidence) and $\langle z \rangle = 5.3$ (95% confidence) for the average redshift of GRB sources in the Einstein–de Sitter cosmology. The values of $\langle z \rangle$ we obtain for our best-fit models (see § 3.1) are all well within these limits. The effective redshift distributions are also consistent with the disparity found by Norris et al. (1995) between the duration distributions of bright and dim GRBs, which they interpret as the signature of cosmological time dilation for a GRB source distribution with the dimmest bursts at $z \approx 2$.

On the other hand, our effective redshift distributions are somewhat at odds with the conclusion of Wijers et al. (1998) that the faintest bursts observed with BATSE are at redshifts of $3 < z < 6$. Part of the discrepancy is explained by the fact that rate model used by Wijers et al. (1998) does not correct for the cosmological time dilation of the comoving burst rate. According to our results with models D1, D2, and D3, no more than 0.002%, 1%, or 5% (respectively) of the bursts observed with our off-line sample are from redshifts larger than $z = 3.0$ and fewer than 8×10^{-7}%, 0.07%, and 0.3%, respectively, are at redshifts greater than $z = 4.0$. Therefore, it is possible that GRBs may be produced at redshifts as high as $z \approx 6$, but even model D3, which allows the highest redshifts, permits only a 7% chance that one or more such bursts have been observed among the 2265 in the off-line sample.

To summarize, our off-line search of archival BATSE data has explored the distribution of GRB intensities at peak fluxes below the onboard detection threshold. We find a paucity of faint bursts detected on the 4.096 and 8.192 s timescales that were not already detected on the 1.024 s timescale. The differential intensity distribution is consistent with models in which the GRB rate traces the global star formation history of the universe, and it is marginally consistent with the model in which the GRB rate is independent of redshift. We argue that the models in which the GRB rate traces the star formation rate are nevertheless preferred, based on the paucity of faint bursts detected exclusively on the 4.096 and 8.192 s timescales and on the comparison of the inferred effective luminosity and redshift distributions with the bursts for which redshifts have been measured. As an application of the off-line GRB intensity distribution, we set a limit of 10% (99% confidence) on the fractional rate of all GRBs that could belong to a homogeneous (in Euclidean space) subpopulation of burst sources (such as Type Ib/c supernovae).

Note added in manuscript.—Stern et al. (1999) recently described preliminary results from their search of the BATSE data for nontriggered GRBs. They use detection criteria nearly identical to ours, yet they identified as GRBs at least 396 transient events (in the time period of our search) that do *not* appear in our nontriggered GRB catalog (B. Stern 1999, private communication). We have visually reexamined all 396 of these events to investigate the discrepancy and to evaluate its possible implications for the results described in this paper.

Out of the 396 events, there were 95 that occurred immediately before or after a data gap. Our off-line trigger is not sensitive during these times because the background average cannot be formed from missing data. The omission of these 95 events cannot affect the rates or model results of this paper because there is no intensity bias against detecting them and the data in which they appear do not contribute to our live-time calculation. There were also eight events in the preliminary version of the Stern et al. catalog that are BATSE onboard triggers, which are excluded from our search by definition.

The classification of the remaining 293 events is subjective. In our work, all off-line triggers were inspected and classified by just one person (J. K.).[10] Upon examining the 293 events that were classified by Stern et al. (1999) as GRBs but as something else by us, we find 32 that we believe to be atmospheric electron precipitation events, 31 that we put in our "unknown" category because they appeared softer than typical GRBs (though they could represent the low-energy tail of the GRB spectral distribution), three events that appear to be solar flares, one event that appears to be a phosphorescence spike, and one event that was already in our nontriggered GRB catalog.

This leaves 213 events in the preliminary list by Stern et al. (1999) that we originally assigned to non-GRB causes. Many of these have ambiguous characteristics: because they were difficult to classify as GRBs with high confidence, we followed our "conservative" classification approach (Kommers et al. 1997) and did not accept them as GRBs. There are also clear cases of human error during our initial classification. We had previously estimated (§ 2.2) that as many as 200 (90% confidence) genuine GRBs could have been missed in our search because of human classification error, and our comparison with the work of Stern et al. has indeed uncovered approximately this many, corresponding to a total "loss rate" for GRBs of ~ 9%.

[10] Out of $\sim 370{,}000$ off-line triggers detected during the off-line search, only $\sim 22{,}000$ are associated with events that we classified as GRBs (a single transient can cause from 2 to greater than 20 off-line triggers depending on its duration and time profile). Since only about 16% of all off-line triggers are associated with GRB causes, we approach the classification of each transient event from the point of view that it is not a GRB, unless all other causes are reasonably excluded.

TABLE 9

DATA FOR FITTING DIFFERENTIAL PEAK FLUX DISTRIBUTION

P_1	P_2	ΔN_{obs}	ΔR (yr^{-1} sr^{-1})
0.180.....	0.202	105	2.96 ± 0.29
0.202.....	0.227	103	2.91 ± 0.29
0.227.....	0.254	108	3.05 ± 0.29
0.254.....	0.285	117	3.30 ± 0.31
0.285.....	0.320	98	2.76 ± 0.28
0.320.....	0.359	104	2.93 ± 0.29
0.359.....	0.403	101	2.84 ± 0.28
0.403.....	0.452	118	3.33 ± 0.31
0.452.....	0.507	97	2.74 ± 0.28
0.507.....	0.569	81	2.29 ± 0.25
0.569.....	0.639	86	2.43 ± 0.26
0.639.....	0.717	93	2.62 ± 0.27
0.717.....	0.804	74	2.09 ± 0.24
0.804.....	0.902	84	2.37 ± 0.26
0.902.....	1.000	54	1.52 ± 0.21
1.000.....	1.259	118	3.33 ± 0.31
1.259.....	1.584	113	3.19 ± 0.30
1.584.....	1.995	104	2.93 ± 0.29
1.995.....	2.511	72	2.03 ± 0.24
2.511.....	3.162	60	1.69 ± 0.22
3.162.....	3.981	49	1.38 ± 0.20
3.981.....	5.011	40	1.15 ± 0.18
5.011.....	6.309	27	0.76 ± 0.15
6.309.....	7.943	26	0.73 ± 0.14
7.943.....	20.00	64	1.81 ± 0.23

We have repeated the model fitting and analysis described in this paper assuming that all 213 of these transients are genuine GRBs. Thus the new burst sample includes our original sample of 2265 bursts, plus the 213 bursts from the Stern et al. catalog. With these new data, the most significant change from our original results is that we find $\langle (C_{min}/C_{max})^{3/2} \rangle = 0.199 \pm 0.006$. While this represents a larger Euclidean $\langle V/V_{max} \rangle$ than is obtained from our original sample, it is still the lowest value yet obtained for a sample of GRBs.

The faint end of the peak flux distribution is changed by the addition of the 213 new events. Table 9 gives the peak flux distribution with these bursts included. For consistency, we derived peak fluxes for the 213 bursts using our software rather than using the peak fluxes provided by Stern (1999, private communication).

Stern et al. (1999) report a significant steepening of the slope of the differential peak flux distribution at peak fluxes between 0.1 and 0.2 photons cm^{-2} s^{-1} in the 50–300 keV band. The reported steepening is most significant below the 0.16 photons cm^{-2} s^{-1} threshold used for our model fitting. Below this threshold the data are subject to large corrections for detection efficiency. Our estimates of the off-line trigger efficiency of our search are subject to systematic errors arising from the assumption that all GRBs are well represented in the 50–300 keV band by a power-law spectral model; therefore, we chose not to fit number counts that are subject to a correction for trigger efficiency of more than a 20%.

Our original sample contained 1998 bursts that had peak fluxes greater than the 0.16 photons cm^{-2} s^{-1} threshold for our analysis. The events from Stern et al. (1999) contribute 98 more bursts above this threshold for a combined sample of 2096 bursts. We find that although the addition of the 98 bursts steepens the slope of the distribution at the faint end (see Table 9) the fitted parameters of our models do not change appreciably.

Table 10 gives the best-fit parameters for cosmological models with a power-law luminosity function, based on the combined sample of 2096 bursts. For all three models the fitted parameters are changed insignificantly relative to the uncertainties.

The comparison of our nontriggered GRB catalog with that of Stern et al. (1999) shows that the classification of faint GRBs in the BATSE data is uncertain and subject to some level of confusion with other sources of radiation in the spacecraft environment. The reliability of the GRB identifications is substantially increased when each candidate GRB is inspected by more than one person, as is standard practice in the BATSE team for onboard burst triggers. Interference from atmospheric electron precipitation events can be a significant source of confusion. Equatorial orbits for future GRB detectors such as HETE-2 will greatly reduce the number of GRBs that can be mistaken for magnetospheric particle precipitations (and vice versa).

Finally, relevant to Figure 5, P. Groot (1999, private communication) has pointed out that the lack of observed redshifts in the range $z \approx 1.5$–2.7 may be due to observational selection. The detectable emission lines in this redshift range are inaccessible to current instrumentation on the Keck telescopes.

J. M. K. thanks Bob Rutledge for a careful reading of the manuscript, and acknowledges useful discussions with Ed Fenimore, Jon Hakkila, Gabriela Marani, Bob Nemiroff, and Ralph Wijers, as well as support from NASA Graduate Student Researchers Program Fellowship NGT8-52816. W. H. G. L. acknowledges support from NASA under grant NAG5-3804. C. K. acknowledges support from NASA under grants NAG5-32490 and NAG5-4799. J. v. P. acknowledges support from NASA under grants NAG5-2755 and NAG5-3674.

TABLE 10

BEST-FIT PARAMETERS FOR COSMOLOGICAL MODELS WITH POWER-LAW LUMINOSITY FUNCTION, USING 213 ADDITIONAL BURSTS FROM STERN ET AL.

$\rho(z)$	R_0 (h_{70}^3 Gpc^{-3} yr^{-1} sr^{-1})	L_{min} (10^{51} h_{70}^{-2} ergs s^{-1})	β	χ^2 (22 d.o.f)
D1 (constant).....	10.4 ± 1.3	0.22 ± 0.10	$3.9_{-1.0}$[a]	21.5
D2 (SFR)	2.5 ± 0.3	0.43 ± 0.2	2.0 ± 0.3	15.3
D3 (AGN)	2.3 ± 0.5	0.83 ± 0.5	2.1 ± 0.5	18.1

[a] This parameter is not constrained above the the best-fit value when the other parameters are free to vary.

REFERENCES

Avni, Y. 1976, ApJ, 210, 642
Band, D., et al. 1993, ApJ, 413, 281
Bloom, J. S., Kulkarni, S. R., Harrison, F., Prince, T., Phinney, E. S., & Frail, D. A. 1998, ApJ, 506, L105
Cohen, E., & Piran, T. 1995, ApJ, 444, L25
Costa, E., et al. 1997, Nature, 387, 793
Djorgovski, S. G., Kulkarni, S. R., Bloom, J. S., Frail, D. A., Chaffee, F., & Goodrich, R. 1999, GCN Circ. 189
Djorgovski, S. G., Kulkarni, S. R., Bloom, J. S., Goodrich, R., Frail, D. A., Piro, L., & Palazzi, E. 1998, ApJ, 508, L17
Dunlop, J. S. 1998, in Observational Cosmology with the New Radio Surveys, ed. M. N. Bremer et al. (Dordrecht: Kluwer), 157
Fall, S. M., Charlot, S., & Pei, Y. C. 1996, ApJ, 464, L43
Fenimore, E. E., & Bloom, J. S. 1995, ApJ, 453, 25
Fenimore, E. E., et al. 1993, Nature, 366, 40
Fishman, G. J., et al. 1989, in Proc. *GRO* Science Workshop (Greenbelt, MD: NASA GSFC), 2-39
———. 1994, ApJS, 92, 229
Frail, D. A., et al. 1997, Nature, 389, 261
Galama, T. J., et al. 1998, Nature, 395, 670
Hakkila, J., et al. 1996, ApJ, 462, 125
Hartmann, D., Blumenthal, G., Chuang, K.-W., Hurley, K., Kargatis, V., Liang, E., & Linder, E. 1992, in Gamma-Ray Bursts Observations, Analyses, and Theories, ed. C. Ho, R. I. Epstein, & E. E. Fenimore (Cambridge: Cambridge Univ. Press), 45
Higdon, J. C., & Schmidt, M. 1990, ApJ, 355, 13
Holz, D. E., Miller, M. C., & Quashnock, J. M. 1998, preprint (astro-ph/9804271)
Horack, J. M., Hakkila, J., Emslie, A. G., & Meegan, C. A. 1996, ApJ, 462, 131
Hughes, D. H., et al. 1998, Nature, 394, 241
in't Zand, J. J. M., & Fenimore, E. E. 1994, in AIP Conf Proc. 307, Gamma-Ray Bursts, ed. G. J. Fishman, J. J. Brainerd, & K. Hurley (New York: AIP), 692
Iwamoto, K., et al. 1998, Nature, 395, 672
Kippen, R. M., et al. 1998, ApJ, 506, L27
Kommers, J. M., Lewin, W. H. G., Kouveliotou, C., van Paradijs, J., Pendleton, G. N., Fishman, G. J., & Meegan, C. A. 1998, in AIP Conf. Proc. 428, Gamma Ray Bursts, ed. C. A. Meegan, R. D. Preece, & T. M. Koshut (New York: AIP), 45
Kommers, J. M., Lewin, W. H. G., Kouveliotou, C., van Paradijs, J., Pendleton, G. N., Meegan, C. A., & Fishman, G. J. 1997, ApJ, 491, 704
Kommers, J. M., Lewin, W. H. G., van Paradijs, J., Kouveliotou, C., Fishman, G. J., & Briggs, M. S. 1996, in AIP Conf. Proc. 384, Gamma Ray Bursts, ed. C. Kouveliotou, M. S. Briggs, & G. J. Fishman (New York: AIP), 441
Kommers, J. M., et al. 1999, ApJ, 511, 514 (erratum 491, 704 [1997])
Koshut, T. M., Paciesas, W. S., Kouveliotou, C., van Paradijs, J., Pendleton, G. N., Fishman, G. J., & Meegan, C. A. 1996, ApJ, 463, 570
Kouveliotou, C., Meegan, C. A., Fishman, G. J., Bhat, N. P., Briggs, M. S., Koshut, T. M., Paciesas, W. S., & Pendleton, G. N. 1993, ApJ, 413, L101
Krumholz, M., Thorsett, S. E., & Harrison, F. A. 1998, ApJ, 506, L81
Kulkarni, S. R., et al. 1998a, Nature, 393, 35
———. 1998b, Nature, 395, 663
Lilly, S. J., Le Fevre, O., Hammer, F., & Crampton, D. 1996, ApJ, 460, L1
Loredo, T. J., & Wasserman, I. M. 1995, ApJS, 96, 261
———. 1997, preprint (astro-ph/9701111)
———. 1998, ApJ, 502, 75
Loveday, J., Peterson, B. A., Efstathiou, G., & Maddox, S. J. 1992, ApJ, 390, 338
Madau, P., Della Valle, M., & Panagia, N. 1998a, MNRAS, 297, L17
Madau, P., Pozzetti, L., & Dickinson, M. 1998b, ApJ, 498, 106
Mallozzi, R. S., Pendleton, G. N., & Paciesas, W. S. 1996, ApJ, 471, 636
Mao, S., & Mo, H. J. 1998, A&A, 339, L1
Marani, G. F., Nemiroff, R. J., Norris, J. P., Hurley, K., & Bonnell, J. T. 1998, in AIP Conf. Proc. 428, Gamma Ray Bursts, ed. C. A. Meegan, R. D. Preece, & T. M. Koshut (New York: AIP), 166
Matz, S. M., Higdon, J. C., Share, G. H., Messina, D. C., & Iadicicco, A. 1992, in Gamma-Ray Bursts Observations, Analyses, and Theories, ed. C. Ho, R. I. Epstein, & E. E. Fenimore (Cambridge: Cambridge Univ. Press), 175
Meegan, C. A., Fishman, G. J., Wilson, R. B., Paciesas, W. S., Pendleton, G. N., Horack, J. M., Brock, M. N., & Kouveliotou, C. 1992, Nature, 355, 143
Meegan, C. A., et al. 1996, ApJS, 106, 65
Metzger, M., et al. 1997, Nature, 387, 878
Norris, J. P., Bonnell, J. T., Nemiroff, R. J., Scargle, J. D., Kouveliotou, C., Paciesas, W. S., Meegan, C. A., & Fishman, G. J. 1995, ApJ, 439, 542
Norris, J. P., Bonnell, J. T., & Watanabe, K. 1998, preprint (astro-ph/9807322)
Ogasaka, Y., Murakami, T., Nishimura, J., Yoshida, A., & Fenimore, E. E. 1991, ApJ, 383, L61
Paciesas, W. S., et al. 1999, ApJS, 122, 465
Press, W., Flannery, B., Teukolsky, S., & Vetterling, W. 1995, Numerical Recipes in C (Cambridge: Cambridge Univ. Press)
Rutledge, R. E., Hui, L., & Lewin, W. H. G. 1995, MNRAS, 276, 753
Schaefer, B. E., Cline, T. L., Hurley, K. C., & Laros, J. G. 1997, ApJ, 489, 693
Schechter, P. 1976, ApJ, 203, 297
Schmidt, M., Higdon, J. C., & Hueter, G. 1988, ApJ, 329, L85
Stern, B., Tikhomirova, Ya., Stepanov, M., Kompaneets, D., Berezhnoy, A., & Svensson, R. 1999, preprint (astro-ph/9903094)
Tinney, C., Stathakis, R., Cannon, R., & Galama, T. J. 1998, IAU Circ. 6896
Totani, T. 1997, ApJ, 486, L71
———. 1998, preprint (astro-ph/9805263)
Ulmer, A., Wijers, R. A. M. J., & Fenimore, E. E. 1995, ApJ, 440, L9
van Paradijs, J., et al. 1997, Nature, 386, 686
Weinberg, S. 1972, Gravitation and Cosmology: Principles and Applications of the General Theory of Relativity (New York: Wiley), 483
Wijers, R. A. M. J., Bloom, J. S., Bagla, J. S., & Natarajan, P. 1998, MNRAS, 294, L13
Woods, E., & Loeb, A. 1995, ApJ, 453, 583
Woods, P., Kippen, R. M., & Connaughton, V. 1998, GCN Circ. 112